



*Dedicated to Academician Cristian Silvestru
on the occasion of his 70th anniversary*

PARADIGM SHIFT IN SILICON–OXYGEN BONDING: A NOVEL ORGANODISILOXANE WITH LINEAR GEOMETRY

Mădălin DĂMOC, Alexandru-Constantin STOICA, Mihaela DASCĂLU,
Sergiu SHOVA and Maria CAZACU*

Department of Inorganic Polymers, “Petru Poni” Institute of Macromolecular Chemistry,
41A Grigore Ghica Voda Alley, 700487 Iasi, Roumania

Received February 26, 2025

An organosiloxane compound, 1,1'((1,1,3,3-tetramethyldisiloxane-1,3-diyl)bis(methylene))bis(*1H*-1,2,3-triazole-4-carboxylic acid), [HOOC–C₂HN₃–CH₂(CH₃)₂Si]₂O·2DMSO, **H₂L**, exhibiting a rare, perfectly linear Si–O–Si bond angle of 180°, and the two carboxyl groups in the *trans* position, as highlighted single-crystal by X-ray diffraction (SCXRD) analysis, was



synthesized via a 1,3-dipolar Huisgen cycloaddition. The structure was also verified by elemental analysis and spectral (FTIR and ¹H, ¹³C NMR) techniques. The calculated values of the Si–O–Si angle, ranging from 165.051° to 179.995°, depending on the imposed restrictions, together with the considerable length of the Si–O bond, both measured (1.6113(9) Å) and calculated (1.6527 Å), do not support a significant double bond character. The linearity can rather be attributed to supramolecular crystal packing interactions. This study contributes to the diversification of organosilicones and to a deeper understanding of the siloxane bond, with implications both in the fundamental chemistry and in the practical applications of this class of compounds.

INTRODUCTION

The Si–O–Si bond underlies a wide range of compounds, including polydiorganosiloxanes (silicones) or small-molecule organosiloxane compounds and inorganic silicates (such as natural silicates and glass), having a defining influence on their properties. The characteristics of this bond have been the focus of extensive theoretical and experimental studies. The dual ionic-covalent

character of the Si–O bond, together with hyperconjugative interactions, such as those of the p(O)→σ*(Si–R) type, found to be dominant,¹ shape the structural and electronic properties of siloxanes, distinguishing them from their ethereal organic analogues^{2,3} and governing the behavior of siloxanes.⁴

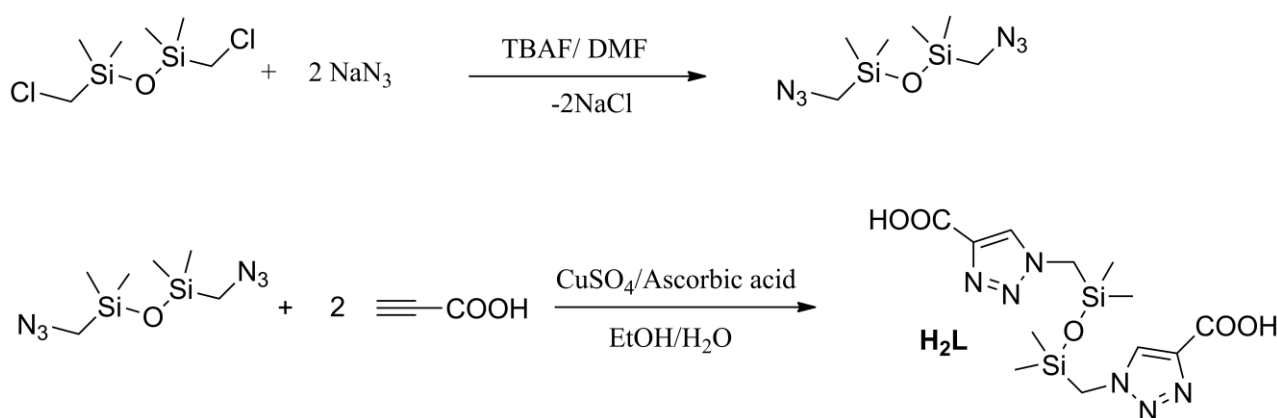
A notable feature of siloxanes is the variability of the Si–O–Si bond length and angle. The latter typically ranges between 130° and 160° in most such

* Corresponding author: mcazacu@icmpp.ro

compounds, significantly influencing their properties. Narrower angles are associated with increased basicity and the ability to form stronger hydrogen bonds, while larger angles are associated with reduced electron-donating capabilities and increased hydrophobicity, the extreme values of the latter being obtained in the case of structures with a perfectly linear Si-O-Si bond angle of 180°. ⁵ Such a configuration is extremely rare and marks a significant paradigm shift in the understanding of silicon-oxygen bonding. Only a few linear disiloxane compounds, (R₃Si)₂O, have been reported, all featuring identical substituents on each silicon (*e.g.*, CH=CH₂, Ph and PhCH₂). ⁶⁻⁸ But the implications of these deviations extend beyond academic curiosity. The ability to tune the Si-O-Si bond angle opens avenues for the rational design of new siloxane compounds and materials with tailored properties, from hydrophobic coatings to highly reactive precursors for catalysis. ⁹ As part of the derivatization of siloxane compounds by functionalization with organic groups, in this work, a telechelic functionalized disiloxane with carboxyl groups was obtained, 1,1'((1,1,3,3-tetramethyldisiloxane-1,3-diyl)bis(methylene))bis(*1H*-1,2,3-triazole-4-carboxylic acid), **H₂L**, using the version of the 1,3-dipolar Huisgen cycloaddition ¹⁰ catalyzed by Cu(I) generated *in situ* by the reduction of anhydrous CuSO₄ with ascorbic acid. ¹¹ The structure of the obtained compound exhibits a perfectly linear Si-O-Si bond, as crystallographic analysis revealed.

RESULTS AND DISCUSSION

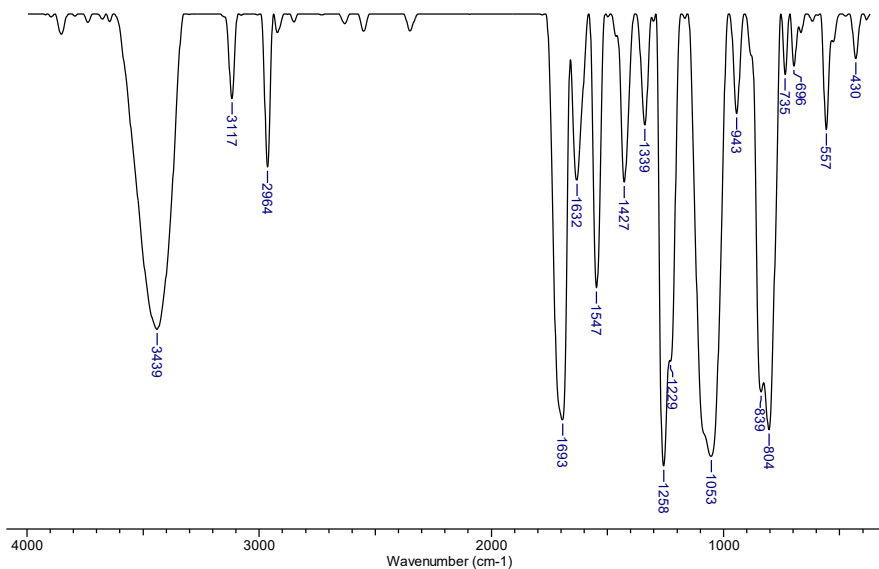
Derivatization of silicones, known for their extreme hydrophobicity, is a key approach for obtaining materials of high industrial importance, such as surfactants, liquid crystals, antifoam agents, etc. But this is often a difficult task due to the large differences in polarity and solubility between the species involved. Traditionally, functionalization processes involve laborious and sometimes inefficient steps, such as protection and deprotection of functional groups, the use of organic solvents and expensive platinum-based catalysts for hydrosilylation. ¹² For the telechelic attachment of carboxylic groups to a disiloxane substrate, here we used Huisgen 1,3-dipolar cycloaddition, also known as Cu(I)-catalyzed “click chemistry”, a robust and efficient method for functionalization of molecules, with the advantage of producing exclusively stable triazole rings, in an environmentally friendly process with high yields, applicable to both molecular and polymer chemistry. ¹⁰ Thus, commercially available 1,3-bis(chloromethyl) tetramethyldisiloxane was treated with NaN₃ in DMF, using tetrabutylammonium fluoride as a phase transfer agent, to give a bis-azide. This was isolated and further reacted with propiolic acid in the presence of a Cu(I) catalyst generated *in situ* by the reduction of anhydrous CuSO₄ with ascorbic acid ¹¹ (Scheme 1).



Scheme 1 – Synthesis of compound **H₂L** via 1,3-dipolar Huisgen cycloaddition.

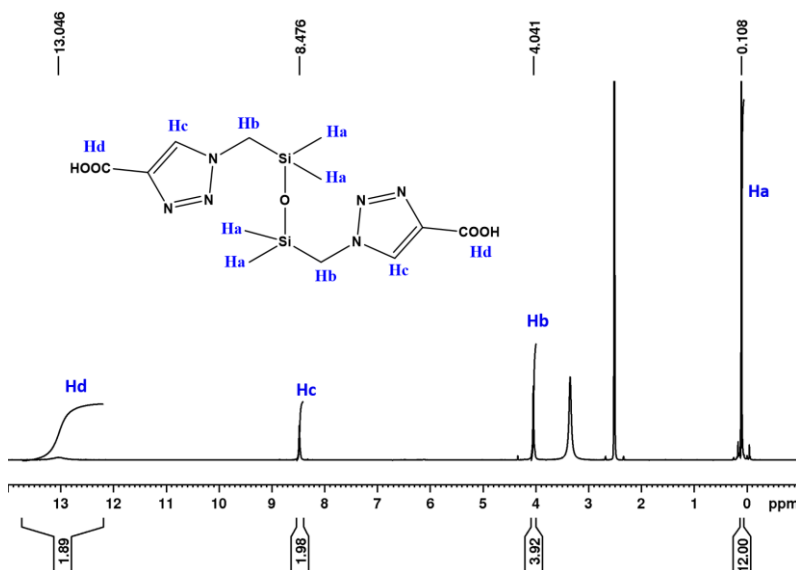
The reaction product, 1,1'((1,1,3,3-tetramethyldisiloxane-1,3-diyl)bis(methylene))bis(*1H*-1,2,3-triazole-4-carboxylic acid), **H₂L**, was isolated by liquid-liquid extraction and subsequent

precipitation from hexane. Its structure was supported by IR and NMR spectroscopy data (Figs. 1–3) and confirmed by single crystal X-ray diffraction (Fig. 4).

Fig. 1 – IR spectrum for **H₂L**.

The FTIR spectrum (Fig. 1) clearly indicates vibrations due to the -COOH group at 1693 cm^{-1} , the 1,2,3 triazole nucleus at 1547 cm^{-1} , and the dimethylsiloxane group at 1258 , 1053 , 839 , and 804 cm^{-1} .¹³ The

^1H NMR spectra (Fig. 2) support the structure of the **H₂L** compound through resonances at 13.04 (COOH), 8.47 (CH), 4.04 (CH_2), 0.10 ppm (Si- CH_3), an argument reinforced by the ^{13}C spectrum (Fig. 3).

Fig. 2 – ^1H NMR spectrum for **H₂L** (DMSO-*d*₆, 400.13 MHz).

Single crystal X-ray analysis on the compound, crystallized from DMSO as white rectangular prisms, revealed the formation of a molecular structure, with the formula $\text{C}_{16}\text{H}_{32}\text{N}_6\text{O}_7\text{S}_2\text{Si}_2$, **[HOOC-C₂HN₃-CH₂Si(CH₃)₂]₂O·2DMSO**, crystallized in the monoclinic system. The crystal structure of this compound is stabilized by hydrogen bonds between two DMSO molecules and the two

carboxyl groups in *trans* position. The asymmetric unit of the compound is given in Fig. 5. The main data about the crystal and data acquisition are presented in Table 1. An intriguing finding from the crystallographic analysis is the perfectly linear Si-O-Si bond angle of 180° . This is rare in the class of these compounds,¹⁴ the most common value being around 145° . A value of 180° for the siloxane

angle would indicate a 100% π bond percentage of the Si-O bond. However, the Si-O bond length is 1.6113(9) Å, very slightly shorter than in other disiloxane compounds, such

as 1,3-bis(carboxypropyl)tetramethyldisiloxane (1.6310(8) Å), where the angle found was 156.2(1),¹⁵ which makes this hypothesis unsustainable.

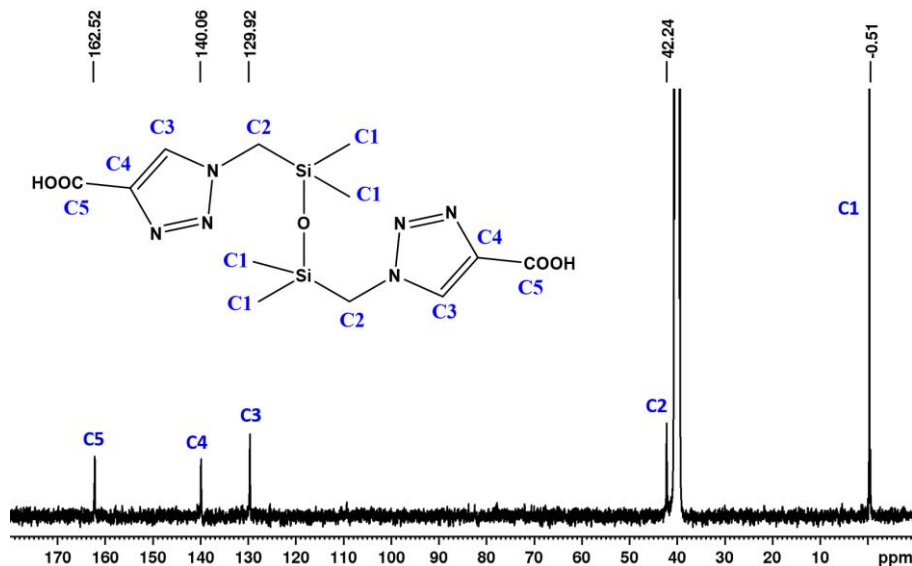


Fig. 3 – ¹³C NMR spectrum for **H₂L** (DMSO-*d*₆, 100.6 MHz).

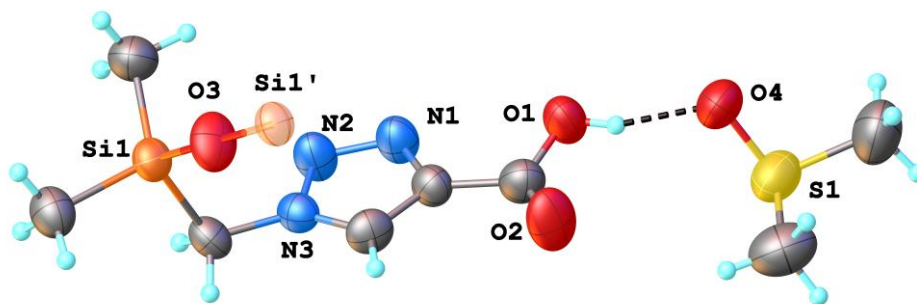


Fig. 4 – X-ray molecular structure for compound **H₂L**. Selected interatomic distances (Å) and angles (°): Si1-O3: 1.6113(9), Si1-C4: 1.884(3), Si1-C5: 1.842(3), Si1-C6: 1.847(3); \angle O3Si1C4: 106.58(11), \angle O3Si1C5: 108.98(12), \angle O3Si1C6: 110.58(12), \angle Si1O3Si1': 180.0; Symmetry code: $^11 - x, -y, 1 - z$.

Table 1

Crystallographic data and data acquisition details for compound **H₂L**.

Identification code	H₂L
Empirical formula, Fw	C ₁₆ H ₃₂ N ₆ O ₇ S ₂ Si ₂ , 540.77
Space group	<i>P2₁/c</i>
<i>a</i> , <i>b</i> , <i>c</i> [Å]	12.7270(9), 6.8689(4), 16.4147(12)
α , β , γ [°]	90, 109.282(8)
Volume [Å ³], <i>Z</i>	1354.49(17), 2
ρ_{calc} [g/cm ³], μ [mm ⁻¹]	1.326, 0.330
Crystal size [mm ³]	0.270 × 0.250 × 0.130
2 θ range for data collection [°]	5.232 to 50.048
Refl. Collected, Indep. Refl., <i>R</i> _{int}	7846, 2358, 0.0650
Data/restraints/parameters	2358/33/173
GOF on <i>F</i> ²	1.014
<i>R</i> ₁ , <i>wR</i> ₂ for [<i>I</i> ≥ 2 σ (<i>I</i>)]	0.0598, 0.0944
<i>R</i> ₁ , <i>wR</i> ₂ for [all data]	0.1155, 0.1179
CCDC No.	2257488

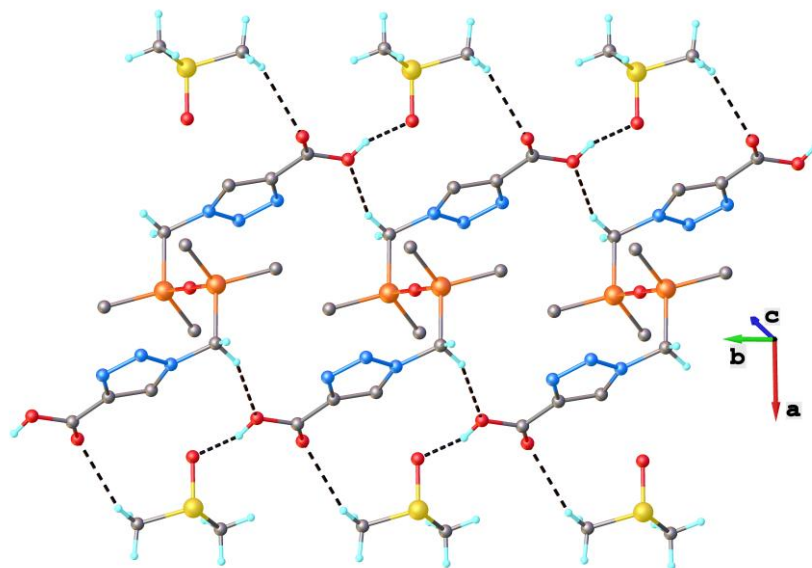


Fig. 5 – View of the 1D strip-like supramolecular array in the crystal of **H₂L**.

Table 2

Hydrogen bonds parameters for **H₂L**.

D-H...A	d(D-H)/Å	d(H-A)/Å	d(D-A)/Å	D-H-A/°	Symmetry code
C4-H...O1	0.97	2.57	3.469(7)	153.7	$x, -1 + y, z$
O1-H...O4	0.82	1.76	2.553(9)	161.5	-
C8-H...O2	0.96	2.51	3.39(2)	151.3	$x, 1 + y, z$

The architecture of this compound features a one-dimensional supramolecular strip (Fig. 5), assembled by intermolecular hydrogen bonds (Table 2). The crystalline structure is constituted by the interpenetration of chains.

Since X-ray diffraction studies on single crystals showed that the oxygen atom is located at the inversion center, having a Si–O–Si angle of 180.0°, theoretical calculations were performed to find the cause of this large value. The structure was optimized using the B3LYP method and the 6-311G(d,p) basis set, both in vacuum and using an implicit model with DMSO. A first optimized molecule in vacuum, **H₂L·2DMSO** (Fig. 6a), yielded a final \angle Si–O–Si value of 178.828°, closely matching the experimentally determined 180.0° from SCXRD, while the Si–O interatomic

distance is 1.6527 Å, slightly higher than the experimentally determined one of 1.6113(9) Å. The optimization process was validated by frequency calculation, as no negative frequencies were found. The calculation results for the optimized **H₂L** molecule itself (Fig. 6b), also validated by the absence of negative frequencies, are similar to those obtained for the co-crystallized DMSO model, namely a \angle Si–O–Si of 179.995° and a Si–O distance of 1.6536 Å. The calculated values for the Si–O interatomic distance are consistent with siloxane bond theory and suggest a partial double bond, as is typical, although the Si–O–Si angle would suggest a full double bond. The images of the HOMO/LUMO orbitals for the optimized molecules are shown in Fig. 7, while their energies are presented in Table 3.

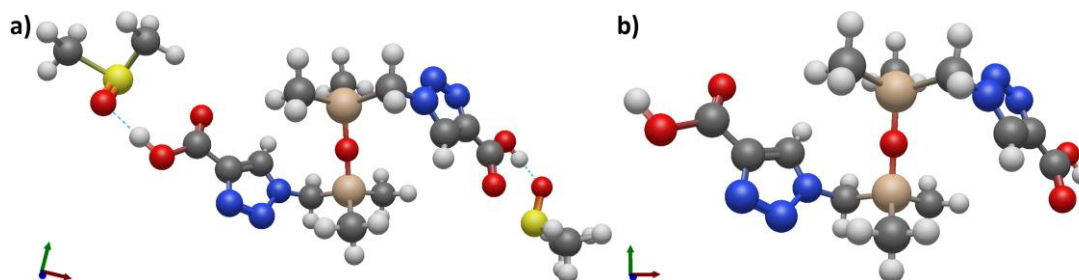


Fig. 6 – Optimized structures in vacuum for: a) **H₂L·2DMSO**; b) **H₂L**.

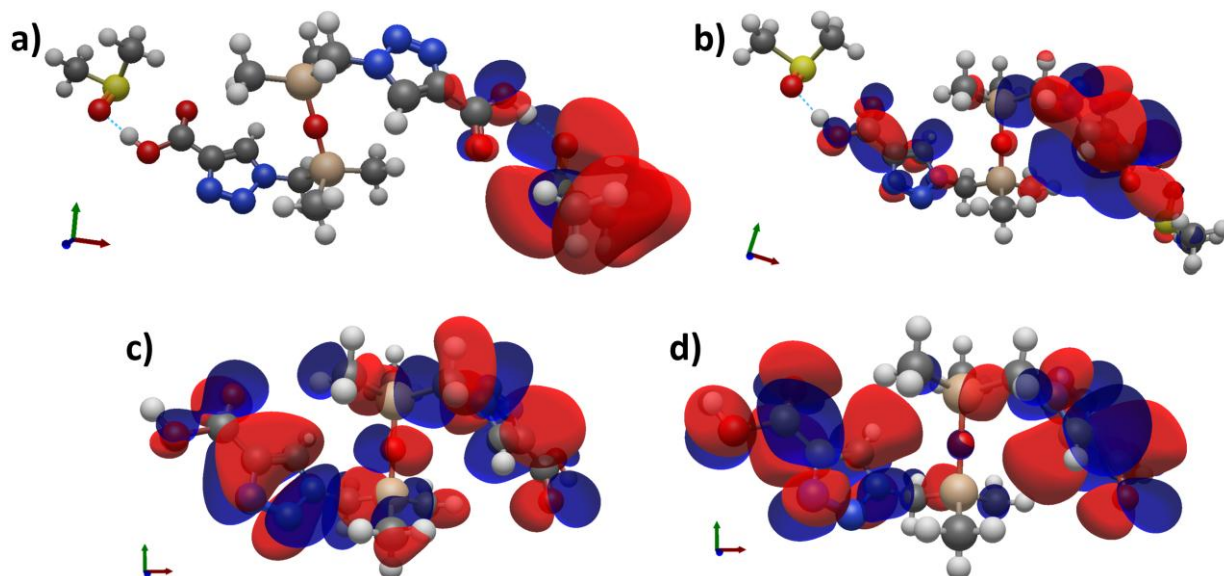


Fig. 7 – HOMO/LUMO images for the vacuum optimized structures: a) $\text{H}_2\text{L}\cdot 2\text{DMSO}$ – HOMO; b) $\text{H}_2\text{L}\cdot 2\text{DMSO}$ – LUMO; c) H_2L – HOMO; d) H_2L – LUMO.

When, for the optimization, an implicit solvent model was applied, with DMSO as the chosen solvent, the result of the calculation this time indicates for the $\text{H}_2\text{L}\cdot 2\text{DMSO}$ molecule (Fig. 8a) a $\angle\text{Si-O-Si}$ value of 165.051° and a Si–O distance of

1.6552 \AA , while for the H_2L molecule (Fig. 8b), a $\angle\text{Si-O-Si}$ angle of 165.256° and a Si–O distance of 1.6551 \AA were calculated. The images of the HOMO/LUMO orbitals are presented in Fig. 9 and their energy values are presented in Table 3.

Table 3

Calculated energies for HOMO/LUMO orbitals				
	Molecule	E_{HOMO}	E_{LUMO}	ΔE (eV)
Vacuum	$\text{H}_2\text{L}\cdot 2\text{DMSO}$	–0.253	–0.025	6.203
	H_2L	–0.274	–0.044	6.258
DMSO	$\text{H}_2\text{L}\cdot 2\text{DMSO}$	–0.258	–0.036	6.040
	H_2L	–0.270	–0.045	6.122

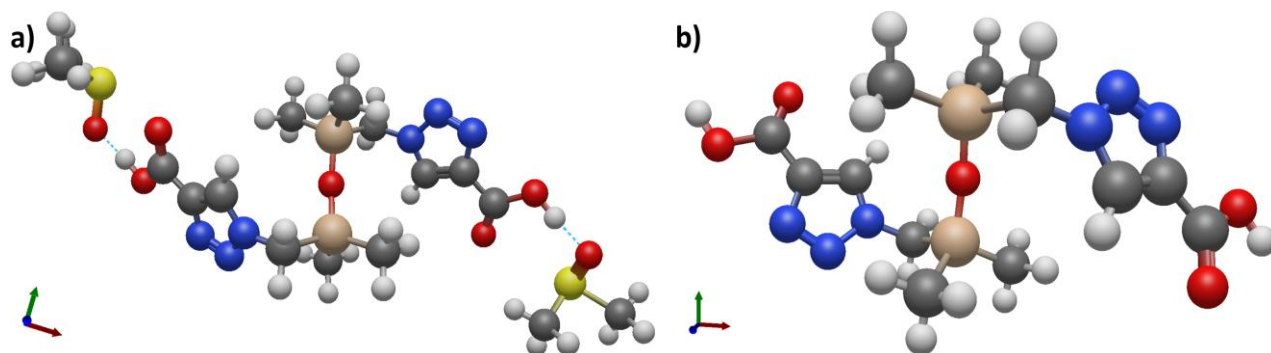


Fig. 8 – Optimized structures using an implicit solvent model with DMSO: a) $\text{H}_2\text{L}\cdot 2\text{DMSO}$; b) H_2L .

Based on the theoretical and experimental results, and taking into account the known flexibility of the Si–O–Si angle, it can be assumed that the increase in its value to 180° , under conditions of high values of the

Si–O bond length, both measured ($1.6113(9)\text{ \AA}$) and calculated (1.6527 \AA), is the effect of intermolecular packing forces in the crystal and not of the increase in the double bond character.

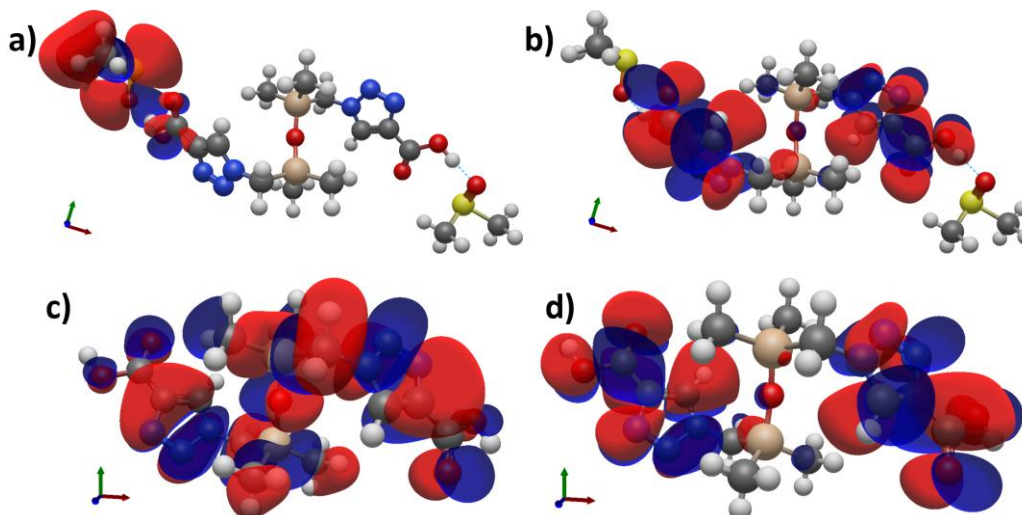


Fig. 9 – HOMO/LUMO images for optimized structures using implicit solvent model with DMSO: a) $\text{H}_2\text{L}\cdot 2\text{DMSO}$ – HOMO; b) $\text{H}_2\text{L}\cdot 2\text{DMSO}$ – LUMO; c) H_2L – HOMO; d) H_2L – LUMO.

EXPERIMENTAL

Materials

Bis(chloromethyl)tetramethyldisiloxane ($\text{C}_6\text{H}_{16}\text{Cl}_2\text{OSi}_2$, M.W. = 231.26, density = 1.05 g/mL, 97 %) from TCI; Tetrabutylammonium fluoride trihydrate ($\text{C}_{16}\text{H}_{42}\text{FNO}_3$, M.W. = 315.51) from Aldrich, sodium azide (NaN_3 , M.W. = 65.01), CuSO_4 from Aldrich, anhydrous Na_2SO_4 from Aldrich, DMF, CHCl_3 , EtOH, DMSO, all solvents used are of chromatographic purity and were purchased from Merck.

Measurements

IR spectra were recorded using a Bruker Vertex 70 FT-IR spectrophotometer in transmission mode at room temperature with a resolution of 2 cm^{-1} and 32 scans. NMR spectra were recorded in $\text{DMSO}-d_6$, on a Bruker Avance NEO 400 MHz spectrometer equipped with a 5 mm direct detection probe, at room temperature. Carbon, hydrogen, nitrogen, and sulfur contents were determined with a Perkin–Elmer CHNS 2400 II elemental analyzer. Crystallographic analysis was performed at 293 K with a Rigaku Oxford-Diffraction XCALIBUR E CCD diffractometer with a $\text{MoK}\alpha$ ($\lambda = 0.71073$) X-ray tube. Unit cell determination and data integration were performed using the CrysAlis¹⁶ software from Oxford Diffraction. The structures were solved using Olex2¹⁷ and SHELXT software¹⁸ and processed by the F^2 least squares matrix with SHELXL-2015¹⁹ using an anisotropic model for all atoms except hydrogen.

Theoretical calculations

Theoretical calculations were performed using the GAUSSIAN 16 and GaussView 6 software. The optimization of the compounds was carried out by using the density functional theory (DFT) method, known as B3LYP, with a 6-311G(d,p) basis set (in its ground state and using the IEFPCM model with DMSO solvent). Avogadro 1.2.0 software was used to create the images.

Synthesis of H_2L

0.3688 g of sodium azide (5.67 mmol) is weighed into a round-bottom flask, after which 20 mL of DMF is added. The temperature is raised to $80\text{ }^\circ\text{C}$, and tetrabutylammonium fluoride trihydrate (10:1) is added. After the temperature reaches the specified value, 0.5 mL (2.27 mmol) of 1,3-*bis*(chloromethyl)tetramethyldisiloxane is added. The mixture is stirred for 12 h at room temperature, then filtered. The solvent is removed from the filtrate by distillation on a rotavap. The remaining solid is dispersed in CHCl_3 , and the insoluble, white fraction is removed by filtration. The filtrate is allowed to evaporate, when a colorless oil remains. This is dissolved in 5 mL of EtOH in a round-bottom flask. Over the solution, 5 mL of water is added, when an emulsion is formed. Over the emulsion is added 281 μL of propargylic acid (4.56 mmol), followed by 40 mg (0.22 mmol) ascorbic acid as a solution in 5 mL of water, and a solution of 5 mg (0.03 mmol) CuSO_4 in 5 mL of water. The mixture is stirred for 48 h at room temperature, after which the solvent mixture is removed on a rotavap,

obtaining a red oil. This oil is dissolved in CHCl_3 , after which liquid-liquid extraction with water is performed three times. The organic fraction is dried on anhydrous Na_2SO_4 . The solvent is evaporated until a minimal amount remains, when hexane is added in excess, obtaining a white precipitate, which is filtered. The product crystallizes from DMSO, as white needles. Yield: 0.27g, 22.0 wt%. IR (KBr), cm^{-1} : ν_{max} 3438s (COOH), 1693s (COOH), 1546s (triazol), 1257vs (Si-CH₃), 1053vs (Si-O-Si), 839s, 804vs (Si-CH₃). ¹H RMN (DMSO-*d*₆, 400.13 MHz): δ (ppm) 13.04 (s, 2H, COOH), 8.47 (s, 2H, C3-H), 4.04 (s, 4H, CH₂), 0.10 (s, 12 H, Si-CH₃). ¹³C RMN (DMSO-*d*₆, 100.6 MHz): δ (ppm) 162.2, 139.88, 129.65, 42.19, -0.26. Anal. Calcd. for $\text{C}_{16}\text{H}_{32}\text{N}_6\text{O}_7\text{S}_2\text{Si}_2$ ($M = 540,77 \text{ g}\cdot\text{mol}^{-1}$), wt %: C 35.54; H 5.96; N 15.54; S 11.86; Found (wt %): C 34.91; H 5.83; N 14.95; S 10.98.

CONCLUSIONS

The reaction of 1,3-bis(chloromethyl) tetramethyldisiloxane with NaN_3 in DMF, followed by the subsequent coupling of the resulting bis-azide with propiolic acid in the presence of an *in situ* generated Cu(I) catalyst, yielded a dicarboxylic acid featuring a tetramethyldisiloxane spacer. Structural analysis revealed a rare, perfectly linear architecture of both fundamental and applied importance. Theoretical calculations, with their restrictions (vacuum modeling or implicit solvent model), depending on the chosen variants, indicate values of the Si-O-Si angle more or less close to the experimental one, but in all cases the Si-O distance is too long to be associated with a 100% double bond. Taking these into account, it seems logical that the linearity of the Si-O-Si angle in this case is the effect of the supramolecular interactions in crystal packing.

Acknowledgement. This work was financially supported by a grant from the Ministry of Research, Innovation and Digitization, project no. PNRR-III-C9-2023-I8-99 within the National Recovery and Resilience Plan.

REFERENCES

1. F. Dankert and C. Hänisch, *Eur. J. Inorg. Chem.*, **2021**, 29, 2907.
2. M. Cypryk and Y. Apeloig, Y. *Organometallics*, **1997**, 16(26), 5938.
3. F. Weinhold and R. West, R., *J. Am. Chem. Soc.*, **2013**, 135(15), 5762.
4. M. Cypryk, J. Kurjata, and J. Chojnowski, *J. Organomet. Chem.*, **2003**, 686(1-2), 373.
5. S. Grabowsky, J. Beckmann, and P. Luger, *Aust. J. Chem.*, **2012**, 65(7), 785.
6. P. D. Lickiss, S. A. Litster, A. D. Redhouse, and C. J. Wisener, *Chem. Commun.*, **1991**, (3), 173.
7. V. E. Shklover, H. B. Bürgi, A. Raselli, T. Armbruster, and W. Hummel, *Acta Crystallogr. B Struct. Sci. Cryst. Eng. Mater.*, **1991**, 47(4), 544.
8. S. M. Haile, and B. J. Wuensch, B. J. *Acta Crystallogr. B Struct. Sci. Cryst. Eng. Mater.*, **2000**, 56(5), 773.
9. B. T. Luke, *J. Phys. Chem.*, **1993**, 97(29), 7505.
10. K. Kacprzak, I. Skiera, M. Piasecka, and Z. Paryzek, *Chem. Rev.*, **2016**, 116(10), 5689.
11. V. V. Rostovtsev, L. G. Green, V. V. Fokin, and K. B. Sharpless, K. B. *Angew. Chem. Int. Ed.*, **2002**, 41(14), 2596.
12. F. Gonzaga, G. Yu, and M. A. Brook, *Chem. Commun.*, **2009**, (13), 1730.
13. D. Cai, A. Neyer, R. Kuckuk and H. M. Heise, *J. Mol. Struct.*, **2010**, 976, 274.
14. C. Glidewell, and D. C. Liles, D. C. *Acta Crystallogr. B Struct. Sci. Cryst. Eng. Mater.*, **1978**, 34(1), 124.
15. M. Cazacu, G. O. Turcan-Trofin, A. Vlad, A. Bele, S. Shova, A. Nicolescu, and A. Bargan, A. *J. Appl. Polym. Sci.*, **2018**, 47144.
16. Rigaku Oxford Diffraction, (2025), CrysAlisPro Software system, version 1.171.44.89, Rigaku Corporation, Wroclaw, Poland
17. O. V. Dolomanov, L. J. Bourhis, R. J. Gildea, J.A.K. Howard and H. Puschmann, *J. Appl. Cryst.* **2009**, 42, 339.
18. G.M. Sheldrick, *Acta Cryst.*, **2015**, A71, 3.
19. G.M. Sheldrick, *Acta Cryst.*, **2015**, C71, 3.